Applied Physics Letters

Voltage-induced modulation in the charge state of Si-vacancy defects in diamond using high voltage nanosecond pulses

Cite as: Appl. Phys. Lett. **119**, 171101 (2021); https://doi.org/10.1063/5.0066537
Submitted: 11 August 2021 • Accepted: 01 October 2021 • Published Online: 25 October 2021

Sizhe Weng, Christopher Coleman, Indu Aravind, et al.

AIP Publishing

Applied Physics Letters ARTICLE scitation.org/journal/apl

Voltage-induced modulation in the charge state of Si-vacancy defects in diamond using high voltage nanosecond pulses

Cite as: Appl. Phys. Lett. **119**, 171101 (2021); doi: 10.1063/5.0066537
Submitted: 11 August 2021 · Accepted: 1 October 2021 ·
Published Online: 25 October 2021

View Online Export Citation CrossMark

Sizhe Weng,[1] Christopher Coleman,[2] Indu Aravind,[3] Yu Wang,[4] Bofan Zhao,[1] and Stephen B. Cronin[1,a)]

AFFILIATIONS

[1]Department of Electrical Engineering, University of Southern California, Los Angeles, California 90089, USA
[2]Nano-Scale Transport Physics Laboratory, School of Physics, University of the Witwatersrand, Private Bag 3, WITS 2050 Johannesburg, South Africa
[3]Department of Physics, University of Southern California, Los Angeles, California 90089, USA
[4]Department of Materials Science, University of Southern California, Los Angeles, California 90089, USA

[a)]Author to whom correspondence should be addressed: scronin@usc.edu

ABSTRACT

Silicon-vacancy defects have been identified as a promising optical transition for quantum communications, quantum control, and quantum information processing. In the work presented here, we demonstrate a voltage-controlled mechanism by which the photoluminescent (PL) emission from silicon-vacancy (Si-V) defects in diamond can be modulated. In particular, we can selectively produce emission from the negatively charged state of this defect (i.e., Si-V^-), which exhibits narrow ($\Gamma = 4$ nm) emission at 738 nm at low laser power. This approach uses high voltage (2–5 kV) nanosecond pulses applied across top and bottom electrodes on a 0.5 mm thick diamond substrate. In the absence of high voltage pulses, we observe no emission at 738 nm. This feature increases monotonically with peak pulse voltage, pulse repetition rate (i.e., frequency), and incident laser intensity. We observe saturation of the PL intensity for pulse voltages above 3.2 kV and frequency above 100 Hz. Based on electrostatic simulations, we estimated the local electric field intensity near the tip of the Cu electrode to be 2.8×10^6 V/cm at these voltages. However, as a function of laser power, we observe a linear dependence of PL intensity without saturation. These saturating and non-saturating behaviors provide important insight into the voltage-induced charging mechanisms and kinetics associated with this process.

Single photon emission from nitrogen-vacancy (NV) centers in diamond has been studied extensively over the past 20 years, as a promising system for realizing secure quantum communication and quantum sensing applications.[1–3] More recently, the silicon-vacancy feature in the luminescence of diamond has been found to be particularly sensitive to the charge state of this defect. In particular, the negatively charged Si-V^- emits at 738 nm,[4–6] whereas the charge neutral (Si-V^0) emits at 946 nm. Unlike NV emission, which is quite broad (~200 nm) at room temperature due to a wide array of phonon sidebands, the Si-V feature is spectrally narrow. These spectrally narrow photons have a high degree of indistinguishability[7] and are better able to couple to photonic crystal cavities and waveguides[8] making them promising candidates for solid-state-based quantum technologies.

Thanks to recent advancements in chemical vapor deposition (CVD) growth techniques, it is now possible to produce isolated Si-V defects in nano-diamond.[9] This has led to a reinvigoration of the field thanks to a significant improvement in photon count rates and optical properties of such samples.[10] To date, single photon emission has been observed from Si-V defects in type IIa CVD diamond,[7] nano-diamonds,[9] and diamond nanowires[11] with g^2 values of 0.26 ± 0.05, ≤ 0.1, and <0.5, respectively. The higher quality samples have also enabled for a deeper understanding of the electronic structure of the Si-V center. The Si-V defect provides a unique molecular structure with the interstitial silicon atom being placed between two unoccupied carbon sites.[12] This results in an inversion symmetry (D_{3d}) of the split-vacancy configuration, which is subsequently responsible for the high spectral stability as it protects the optical transition from local electric field fluctuations.[13] Studies of the electronic structure of the defect have revealed an $S = 1$ ground state for the neutral Si-V^-[14] and an $S = 1/2$ ground state for the negative configuration,[6] where the

zero phonon lines (ZPL) correspond to the wavelengths of 946 and 738 nm, respectively. Furthermore, probing of the Si-V- ZPL through photoluminescence experiments at cryogenic temperatures has revealed a characteristic well-resolved four-line fine structure, as a result of intrinsic spin–orbit-coupling and a dynamic Jahn–Teller effect.[15] Since these properties are especially favorable for developing quantum-based technologies, much research has been directed toward the development of techniques to enhance or refine the initialization, readout, and control of Si-V defects and their incorporation into solid-state devices.

All-optical state initialization, readout, and coherent preparation has been demonstrated and used to establish the Si-V as an excellent platform and spin–photon interface in quantum information processing (QIP).[16] Using a coherent-population trapping technique, the coherent preparation of dark superposition states with a spin coherence time of $T_2^* = 35 \pm 3$ ns was reported.[17] Subsequent work using a combination of optically detected magnetic resonance (ODMR) and microwave coherent control allowed for an enhanced T_2^* of 115 ± 9 ns. By evaluating the temperature dependence of this enhanced spin coherence, the dephasing and decay of the spin state was established to result from a single-phonon-mediated excitation between orbital branches of the ground state of the system.[18] As these findings indicated that the electronic spin coherence was fundamentally limited by orbital relaxation, the possibility of improving state coherence through more refined experimental measurement and control techniques has been the focus of much recent work.[19,20] Sohn *et al.* used strain engineering techniques for improving control and tuning of the Si-V defect.[21] It has recently been shown that the local strain in the Si-V environment can be controlled when fabricated into a nano-electro-mechanical (NEMS) system.[22] This allows for a unique method of tuning of the electronic levels, finer control protocols, and eventually suppression of the interaction between spin and the thermal phonon bath.

While there have been many all-optical studies of photon emission in diamond-defect materials systems, there have been relatively few on their electro-optic or optoelectronic effects. However, in order to utilize these quantum emitters in practical systems it may be necessary to further develop and refine, state initialization, readout and control schemes using electronic means. This could allow for powerful measurement techniques, such as RF reflectometry to complement optical device control. Demonstrating more refined electronic control capabilities may also provide a means for integration with other solid state technologies, providing a stepping stone to scaling up these systems for applications in quantum information processing. Here, we report a voltage-induced switching effect by applying nanosecond high voltage pulses across a diamond film that is able to control the charge state of the Si-V. It is important to note that this effect is not seen with DC voltages of the same magnitude (i.e., up to 5 kV). A systematic study of this voltage-pulse enabled Si-V^- photoluminescence is performed as a function of peak pulse voltage and a pulse repetition rate, in order to understand this switching mechanism.

In this work, polycrystalline type IIa CVD diamond (Element Six, Ltd.) was used with no further processing. Figure 1(b) shows a schematic diagram of the experimental setup in which strips of copper tape that are hand cut to form sharp tips are attached on the top and bottom of the diamond substrate. A tip radius of 20 μm was measured via optical microscopy. Here, the sharp tip of the electrodes provides local field enhancement of the applied electric field across the diamond sample. Two electrodes are separated by 0.5 mm in the lateral direction, and a 532 nm CW laser is focused in between this gap through a long working distance objective lens with $NA = 0.6$. The bottom electrode is connected to a pulse generator (SSPG-20X, Transient Plasma Systems, Inc.), which produces high-voltage pulses with a 5–10 ns rise time ($dV/dt = 10^{12}$ V/s) at a pulse repetition rate of 1–1000 Hz. The typical output characteristics of the nanosecond pulse applied to the bottom electrode are shown in Fig. 1(a), and the top electrode is grounded. Photoluminescence (PL) spectra were collected from the top surface of the diamond sample at the tip of the top electrode using an *inVia* micro-spectrometer (Renishaw, Inc.).

In order to find the electric field distribution around the tip of the Cu electrode, we have performed static simulations using the electrostatic physics package in the AC/DC module available in the COMSOL Multiphysics solutions. The geometry used in the simulation is illustrated in Fig. S1 of the supplementary material. Here, a $10 \times 10\,\text{mm}^2$ diamond sample with 0.5 mm thickness is simulated with triangular shape Cu electrodes on geometrically opposite flat sides. The Cu tip has a terminating curvature of 20 μm. The Cu tip at the top of the diamond is set as ground, and the bottom electrode is set as the high voltage terminal for the simulation. A 3 kV potential is applied to the terminal. We have used the physics-optimized mesh to the system with tetrahedral meshes having a minimum mesh size of 3 μm and a maximum mesh size of 300 μm. Figure 1(d) shows a plot of the electric field profile obtained across the top surface of the diamond sample. Under 3.2 kV excitation, the peak field at the tip of the Cu electrode is 2.8×10^6 V/cm.

Interestingly, the PL signature of the negative state (i.e., Si-V^-) is found to be triggered by a threshold minimum pulse voltage of 3.2 kV. Figure 1(c) shows the PL spectrum of this sample under excitation with 5 kV pulses at a repetition rate of 100 Hz (laser power = 37 μW). Here, we observe three peaks superimposed on the broad NV photoluminescent background. The peaks at 575 and 637 nm correspond to NV and are not electrically active. The peak at 738 nm, however, corresponds to the Si-V^- defect and is only observed under excitation with high voltage nanosecond pulses. In addition, the difference in the NV background is attributed to the Stark effect that the E-field could be very large.[23,24]

In order to understand the voltage-activation of Si-V^- state emission at 738 nm, we performed a systematic study over a wide range of peak pulse voltages, incident laser powers, and pulse repetition rates (i.e., frequencies). Figure 2(a) shows the background-subtracted spectrum, which exhibits the Si-V^- emission centered around 738 nm with a FWHM of 4 nm. The inset shows a plot of this Si-V^- feature plotted as a function of the incident laser power, which shows a linear dependence without saturation. Figure 2(b) shows the integrated PL intensity (integrated peak area at 738 nm) plotted as a function of peak pulse voltage at three different laser powers (37, 240, and 1020 μW). Here, we see a clear saturation behavior in which the plateau intensity increases with the increasing laser power. That is, the 738 nm emission increases with the increasing peak voltage up to approximately 2–3 kV, above which it reaches a saturation point. Here, we believe that electrons are injected from the electrode driving a transition from Si-V to Si-V^-. Figure 2(c) shows a comparison of the Si-V^- emission and the NV emission showing that while there is a slight shift in this peak, there is no significant change in the integrated intensity of the

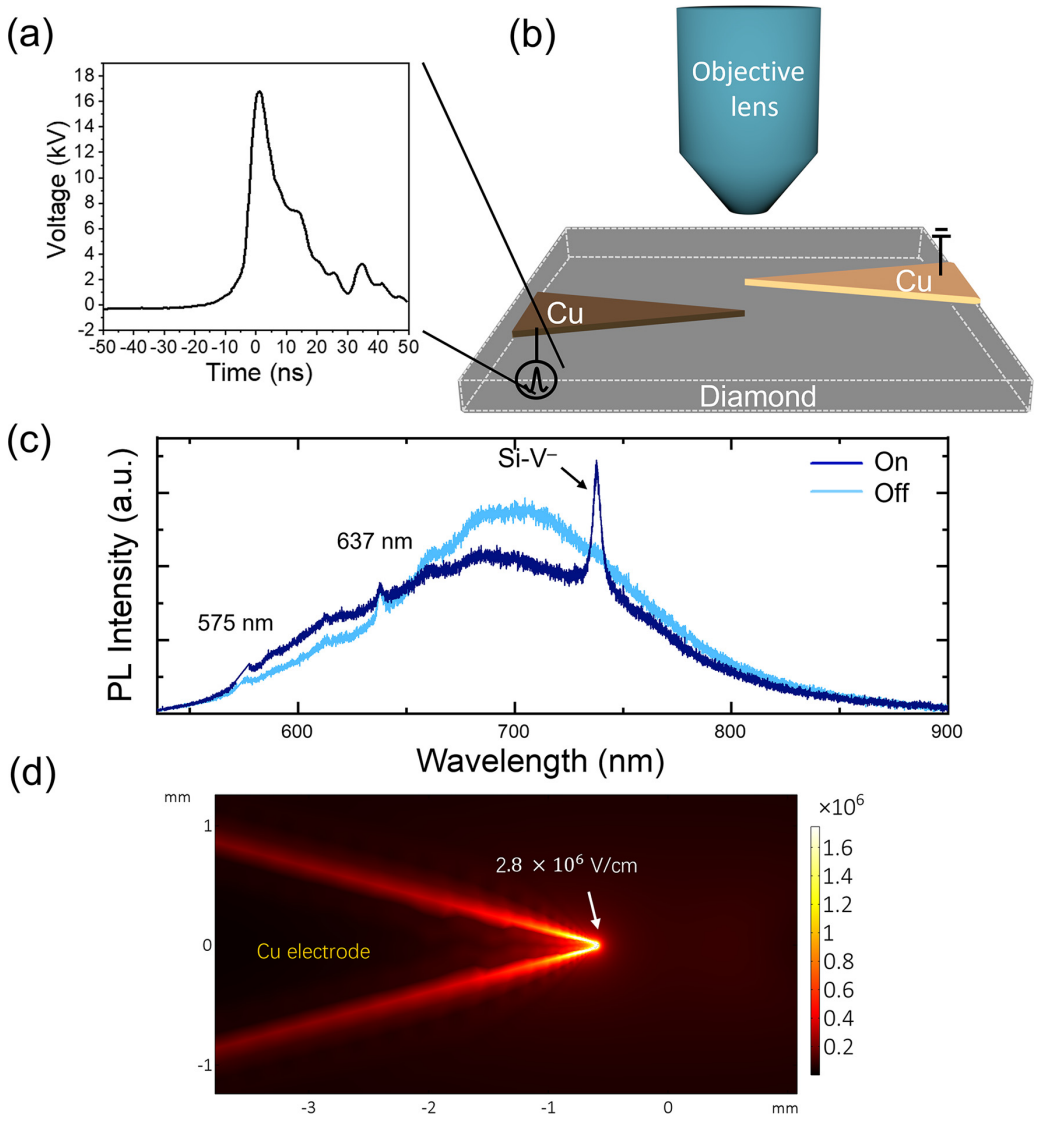

FIG. 1. (a) Typical waveform of our nanosecond high voltage pulse. (b) Schematic diagram of the discharge applied during photoluminescence measurements. (c) Typical PL spectrum for the voltage-activated device. When pulsed to the on state, the Si-V peak at 738 nm is pronounced, also visible are minor peaks associated with nitrogen defect centers (both neutral and the negatively charged states). (d) A plot of the electric field profile obtained across the top surface of the diamond sample.

NV peak with voltage. Figure 2(d) shows a schematic diagram illustrating the high voltage-induced electron injection followed by photoluminescence.

Figure 3 shows the frequency dependence (i.e., pulse repetition rate) of the Si-V^- PL emission at a peak voltage of 5.5 kV. Figure 3(b) shows the background-subtracted spectra from 1 Hz to 1 kHz. Here, there is a sharp increase in PL intensity from 1 to 100 Hz followed by saturation over the 200–1000 range, as plotted in Fig. 3(c). As mentioned above, we performed a control experiment with DC voltages only, and this Si-V^- feature was not observed. Here, turning on the DC voltage only results in one charging event and is essentially equivalent to zero frequency. As such in Fig. 3(c), the PL intensity of the Si-V^- feature drops to zero at $f = 0$. These high voltages can overcome the large Schottky barrier at the copper/diamond interface, injecting charge, and resulting in the SiV- charge state. The saturation around 100 Hz is surprisingly low and indicates that these dynamics are extremely ~10 ms. The decay back to the charge neutral state does not occur via photoemission. Instead, it decays back to zero charge via a slow hopping mechanism from one sub-bandgap defect state to another on the order of 10 ms. Figure S2 in the supplementary material shows a complete set of 66 spectra taken systematically as a function of peak pulse voltage (from 2 to 5.5 kV) and incident laser power (from 2.5 to 1020 μW). Above a pulse peak voltage of 2.5 kV, the intensity of this Si-V^- emission increases, even in the case of

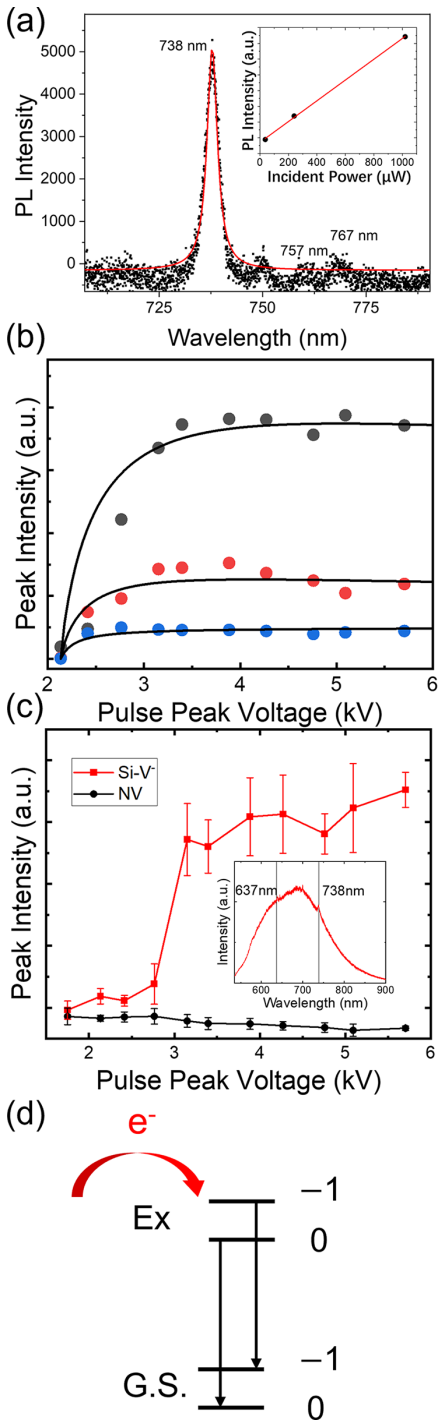

FIG. 2. (a) Si-V$^-$ ZPL at 738 nm, which shows a linear dependence on the incident laser power. (b) Pulse peak voltage-dependence of the PL intensity of the Si-V$^-$ feature exhibiting saturation behavior around 3 kV. (c) Voltage dependence of the Si-V$^-$ and NV emission, showing that the NV emission does not change with pulse peak voltage. (d) Energy diagram of this Si-V defect, the photoexcited state (Ex), and ground state (GS) of the Si-V defect illustrating the high voltage-induced electron injection.

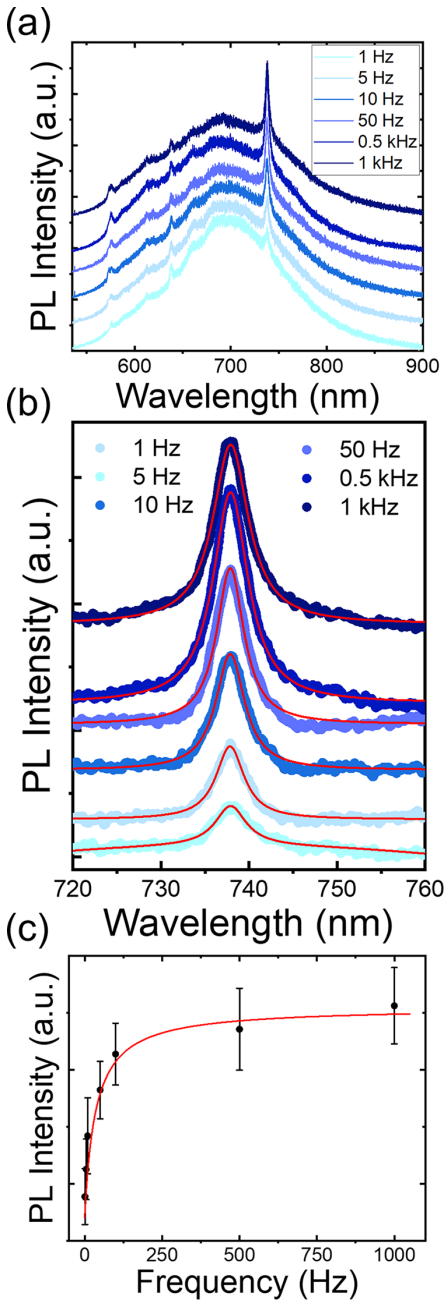

FIG. 3. (a) Raw PL spectra and (b) background-subtracted PL spectra taken with 5.5 kV nanosecond pulses for various pulse repetition rates. (c) Frequency dependence of the PL intensity.

high optical power density. That is, at high optical power densities (~37 μW), there are two separate mechanisms of Si-V$^-$ light emission: one entailing the photo-excitation of the Si-V$^-$ state and another entailing the voltage-induced Si-V$^-$ state. This effect is perhaps best shown in Fig. S3, which presents a summary of the 66 data points plotted in Fig. S2.

In conclusion, we have observed a voltage-induced modulation in the charge state of Si-vacancy defects in diamond using high voltage nanosecond pulses. These negatively charged defects produce spectrally narrow ($\Gamma = 4$ nm) emission centered around 738 nm. The emission intensity increases monotonically with incident laser power, peak pulse voltage, and a pulse repetition rate. No Si-V^- emission is seen at 738 nm without high voltage pulse excitation at low laser powers. Si-V^- emission is only seen above a minimum threshold voltage of 2 kV, which corresponds to a local field intensity of $E = 1.7 \times 10^6$ V/cm. The PL intensity from this Si-V^- defect increases linearly with incident laser power over the range from 37 μW to 1 mW. The PL intensity also increases with peak pulse voltage and a pulse repetition rate. However, the 738 nm PL intensity saturates above 3.2 kV and for the pulse repetition rate above 100 Hz. No Si-V^- emission is observed with DC voltages up to 5.5 kV, indicating that this mechanism of voltage-controlled emission is related to the transient transfer of electrons to the Si-V defect.

See the supplementary material for electric field simulation details and data set of spectra taken as a function of peak pulse voltage and incident laser power.

This research was supported by the Army Research Office (ARO) Award No. W911NF1910257 (S.W.), National Science Foundation (NSF) Award No. CHE-1954834 (I.A.), and Air Force Office of Scientific Research (AFOSR) Grant No. FA9550-19-1-0115 (B.Z.).

DATA AVAILABILITY

The data that support the findings of this study are available from the corresponding author upon reasonable request.

REFERENCES

[1]I. Aharonovich, S. Castelletto, D. Simpson, C. Su, A. Greentree, and S. Prawer, "Diamond-based single-photon emitters," Rep. Prog. Phys. **74**(7), 076501 (2011).
[2]M. W. Doherty, N. B. Manson, P. Delaney, F. Jelezko, J. Wrachtrup, and L. C. L. Hollenberg, "The nitrogen-vacancy colour centre in diamond," Phys. Rep. **528**(1), 1–45 (2013).
[3]Y. Doi, T. Makino, H. Kato, D. Takeuchi, M. Ogura, H. Okushi, H. Morishita, T. Tashima, S. Miwa, S. Yamasaki, P. Neumann, J. Wrachtrup, Y. Suzuki, and N. Mizuochi, "Deterministic electrical charge-state initialization of single nitrogen-vacancy center in diamond," Phys. Rev. X **4**(1), 011057 (2014).
[4]B. L. Green, M. W. Doherty, E. Nako, N. B. Manson, U. F. S. D'Haenens-Johansson, S. D. Williams, D. J. Twitchen, and M. E. Newton, "Electronic structure of the neutral silicon-vacancy center in diamond," Phys. Rev. B **99**(16), 161112 (2019).
[5]T. Müller, C. Hepp, B. Pingault, E. Neu, S. Gsell, M. Schreck, H. Sternschulte, D. Steinmüller-Nethl, C. Becher, and M. Atatüre, "Optical signatures of silicon-vacancy spins in diamond," Nat. Commun. **5**(1), 4328 (2014).
[6]L. J. Rogers, K. D. Jahnke, M. W. Doherty, A. Dietrich, L. P. McGuinness, C. Müller, T. Teraji, H. Sumiya, J. Isoya, N. B. Manson, and F. Jelezko, "Electronic structure of the negatively charged silicon-vacancy center in diamond," Phys. Rev. B **89**(23), 235101 (2014).
[7]A. Sipahigil, K. D. Jahnke, L. J. Rogers, T. Teraji, J. Isoya, A. S. Zibrov, F. Jelezko, and M. D. Lukin, "Indistinguishable photons from separated silicon-vacancy centers in diamond," Phys. Rev. Lett. **113**(11), 113602 (2014).
[8]A. Sipahigil, R. E. Evans, D. D. Sukachev, M. J. Burek, J. Borregaard, M. K. Bhaskar, C. T. Nguyen, J. L. Pacheco, H. A. Atikian, and C. Meuwly, "An integrated diamond nanophotonics platform for quantum-optical networks," Science **354**(6314), 847–850 (2016).
[9]E. Neu, D. Steinmetz, J. Riedrich-Möller, S. Gsell, M. Fischer, M. Schreck, and C. Becher, "Single photon emission from silicon-vacancy colour centres in chemical vapour deposition nano-diamonds on iridium," New J. Phys. **13**(2), 025012 (2011).
[10]A. A. Basov, M. Rähn, M. Pärs, I. I. Vlasov, I. Sildos, A. P. Bolshakov, V. G. Golubev, and V. G. Ralchenko, "Spatial localization of Si-vacancy photoluminescent centers in a thin CVD nanodiamond film," Phys. Status Solidi (a) **206**(9), 2009–2011 (2009).
[11]L. Marseglia, K. Saha, A. Ajoy, T. Schröder, D. Englund, F. Jelezko, R. Walsworth, J. L. Pacheco, D. L. Perry, E. S. Bielejec, and P. Cappellaro, "Bright nanowire single photon source based on SiV centers in diamond," Opt. Express **26**(1), 80 (2018).
[12]J. P. Goss, R. Jones, S. J. Breuer, P. R. Briddon, and S. Öberg, "The twelve-line 1.682 eV luminescence center in diamond and the vacancy-silicon complex," Phys. Rev. Lett. **77**(14), 3041–3044 (1996).
[13]C. Hepp, T. Müller, V. Waselowski, J. N. Becker, B. Pingault, H. Sternschulte, D. Steinmüller-Nethl, A. Gali, J. R. Maze, M. Atatüre, and C. Becher, "Electronic structure of the silicon vacancy color center in diamond," Phys. Rev. Lett. **112**(3), 036405 (2014).
[14]S. S. Moliver, "Electronic structure of neutral silicon-vacancy complex in diamond," Tech. Phys. **48**(11), 1449–1453 (2003).
[15]J. C. A. Prentice, B. Monserrat, and R. J. Needs, "First-principles study of the dynamic Jahn-Teller distortion of the neutral vacancy in diamond," Phys. Rev. B **95**(1), 014108 (2017).
[16]J. R. Weber, W. F. Koehl, J. B. Varley, A. Janotti, B. B. Buckley, C. G. Van De Walle, and D. D. Awschalom, "Quantum computing with defects," Proc. Natl. Acad. Sci. **107**(19), 8513–8518 (2010).
[17]L. J. Rogers, K. D. Jahnke, M. H. Metsch, A. Sipahigil, J. M. Binder, T. Teraji, H. Sumiya, J. Isoya, M. D. Lukin, P. Hemmer, and F. Jelezko, "All-optical initialization, readout, and coherent preparation of single silicon-vacancy spins in diamond," Phys. Rev. Lett. **113**(26), 263602 (2014).
[18]B. Pingault, D.-D. Jarausch, C. Hepp, L. Klintberg, J. N. Becker, M. Markham, C. Becher, and M. Atatüre, "Coherent control of the silicon-vacancy spin in diamond," Nat. Commun. **8**(1), 15579 (2017).
[19]D. D. Sukachev, A. Sipahigil, C. T. Nguyen, M. K. Bhaskar, R. E. Evans, F. Jelezko, and M. D. Lukin, "Silicon-vacancy spin qubit in diamond: A quantum memory exceeding 10 ms with single-shot state readout," Phys. Rev. Lett. **119**(22), 223602 (2017).
[20]J. N. Becker, B. Pingault, D. Groß, M. Gündoğan, N. Kukharchyk, M. Markham, A. Edmonds, M. Atatüre, P. Bushev, and C. Becher, "All-optical control of the silicon-vacancy spin in diamond at millikelvin temperatures," Phys. Rev. Lett. **120**(5), 053603 (2018).
[21]Y.-I. Sohn, S. Meesala, B. Pingault, H. A. Atikian, J. Holzgrafe, M. Gündoğan, C. Stavrakas, M. J. Stanley, A. Sipahigil, J. Choi, M. Zhang, J. L. Pacheco, J. Abraham, E. Bielejec, M. D. Lukin, M. Atatüre, and M. Lončar, "Controlling the coherence of a diamond spin qubit through its strain environment," Nat. Commun. **9**(1), 2012 (2018).
[22]S. Meesala, Y.-I. Sohn, B. Pingault, L. Shao, H. A. Atikian, J. Holzgrafe, M. Gündoğan, C. Stavrakas, A. Sipahigil, C. Chia, R. Evans, M. J. Burek, M. Zhang, L. Wu, J. L. Pacheco, J. Abraham, E. Bielejec, M. D. Lukin, M. Atatüre, and M. Lončar, "Strain engineering of the silicon-vacancy center in diamond," Phys. Rev. B **97**(20), 205444 (2018).
[23]E. Van Oort and M. Glasbeek, "Electric-field-induced modulation of spin echoes of N-V centers in diamond," Chem. Phys. Lett. **168**(6), 529–532 (1990).
[24]T. Mittiga, S. Hsieh, C. Zu, B. Kobrin, F. Machado, P. Bhattacharyya, N. Z. Rui, A. Jarmola, S. Choi, D. Budker, and N. Y. Yao, "Imaging the local charge environment of nitrogen-vacancy centers in diamond," Phys. Rev. Lett. **121**(24), 246402 (2018).